Inorganic Chemistry

ARTICLE

pubs.acs.org/IC

Chromic Behaviors of Hexagonal Columnar Liquid Crystalline Platinum Complexes with Catecholato, 2-Thiophenolato, and Benzenedithiolato

Ho-Chol Chang,*[,†] Kazuki Komasaka,[†] Keisuke Kishida,[‡] Tomoki Shiozaki,[‡] Takeshi Ohmori,[‡] Takeshi Matsumoto,[†] Atsushi Kobayashi,[†] Masako Kato,[†] and Susumu Kitagawa[‡,§,∥]

[†]Division of Chemistry, Faculty of Science, Hokkaido University, North 10, West 8, Kita-ku, Sapporo 060-0810, Japan

[‡]Department of Synthetic Chemistry and Biological Chemistry, Graduate School of Engineering, Kyoto University, Katsura, Nishikyo-ku, Kyoto 615-8510, Japan

[§]ERATO Kitagawa Integrated Pores Project, Japan Science and Technology Agency (JST), Kyoto Research Park Building 3, Shimogyo-ku, Kyoto 600-8815, Japan

[∥]Institute for Integrated Cell-Material Sciences (iCeMS), Kyoto University, Yoshida, Sakyo-ku, Kyoto 606-8501, Japan

Supporting Information

ABSTRACT: Liquid crystalline (LC) platinum(II) complexes with 1,2-thiophenolato and 1,2-benzendithiolato have been newly synthesized and investigated by spectroscopy together with the catecholato analogue. The variations in coordinating atoms (O or S or O/S mixed) lead to significant modulation in electrochemical properties in solution and absorption and emission properties of the complexes both in solution media and in the condensed phases. The asymmetric, polar mesogens/chromophores consisting of Pt(II), redox-active ligands, and alkyl-substituted bipyridine commonly play important roles not only in stabilizing the columnar LC phases, but also in fluctuations of the ground state energies. A key finding of the present work is the chromic properties of LC complexes induced by the interplay of self-association of the mesogens/chromophores and their fluctuating properties.

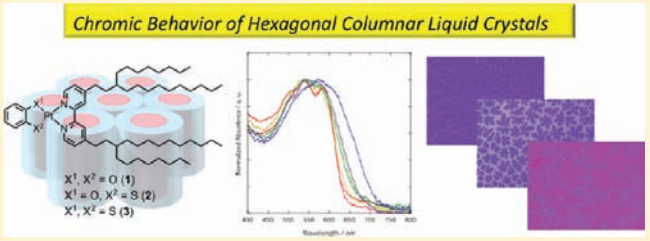

INTRODUCTION

Metal-containing liquid crystals (LCs), metallomesogenes, have been known to show intriguing optoelectronic properties derived from the coexistence of fluctuating physical structures of an LC and a metal/ligand having magnetism, visible light absorption, and emission properties.[1,2] The synergy of functional metal/ligand moieties with LC structures opens a powerful supramolecular approach toward the design of new soft materials.[2] In particular, an LC with an electronically active core is of great interest for unsealing electronic functions such as electrochromic, photovoltaic, and conducting properties, even in LC phases.[3] For example, it is expected that an electronic perturbation induced by oxidation and/or reduction of an LC phase causes well-defined changes in the charged state of molecules, leading not only to the transformation of molecular states, but also to concomitant transformations of macroscopic states through the perturbed intermolecular interactions.

An LC Pt complex, [Pt(Cat)(C8,10bpy)] (**1**), shown in Scheme 1 was designed by our group.[3a] The combination of a redox-active catecholato (Cat)[4] with 3-octyl-tridecyl-4,4′-bipyridine (C8,10bpy) led to the successful formation of a hexagonal columnar ordered LC phase (Col_{ho}) at ambient temperature and up to 195 °C, keeping with the single columnar phase. An asymmetric molecular shape of the complex resulted in a large dipole moment, thereby a one-dimensional columnar structure was formed in which each molecule stacked to cancel out the dipole moment with those of the neighboring molecules. Each column was surrounded by molten alkyl chains and further constructed a two-dimensional hexagonal lattice to form the Col_{ho} phases. One of the noteworthy characteristics of the LC complex is that it showed a direct one-electron oxidation process of Cat to semiquinonato (SQ) not only in solution media but also for the Col_{ho} phase, which was confirmed by the cyclic voltammetric technique for the first time.[3a]

The advantage of our design for redox-active LCs is the fact that structural and electronic properties are controllable by tuning a central mesogen, consisting of a metal ion, a redox-active ligand, and an alkyl-containing ligand. In this paper, we focused our interest on the structural and electronic roles of coordinating atoms. The coordinating atoms within a redox-active ligand might play a primal role in governing, for example, the ligand-field, optical absorption/emission, and redox properties of a molecule.[5,6] In addition to the intramolecular effects of

Received: October 21, 2010
Published: April 20, 2011

Scheme 1. Molecular Structures of Redox-Active Liquid Crystals 1−3

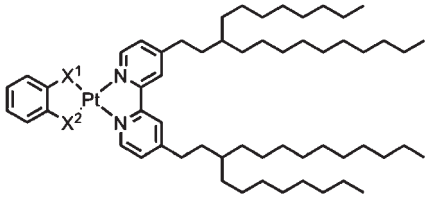

X^1, X^2 = O (**1**)
X^1 = O, X^2 = S (**2**)
X^1, X^2 = S (**3**)

coordinating atoms, they might perturb long-range intermolecular interactions, in particular, in the Col_{ho} phase, because there is a direct interaction between the mesogens in the columnar structures. In this study, two LC complexes possessing 2-thiophenolato (Htp) and 1,2-benzendithiolato (Bdt) were newly synthesized and characterized spectrochemically together with the parent Cat complex (Scheme 1). The different coordinating atoms, O (Cat), O/S (Htp), and S (Bdt), in **1**, **2**, and **3** are expected to tune the molecular and assembled states because of the differences between O and S in size, electronegativity, and bonding interaction with Pt(II). Therefore, it is of interest to clear the relationship between the assembled structures and spectroscopic properties derived from the mesogens/chromophores with differing coordination atoms that would be affected differently by chemical and physical stimuli. In particular, a series of complexes formulated as [Pt(Bdt)(bpy)], where bpy is 2,2′-bipyridine, were intensively investigated for use in photosensitizers for solar cells, in nonlinear optical materials, and in the sensitization of excited oxygen, because of their characteristic absorption of visible light accompanied with luminescence from the long-lived excited states.[7−9] The previous study clearly demonstrated the photoelectrochemical properties of the chromophores in solution and in the solid phases, but those of LC have not been investigated yet. In this paper, the LC structures of new Pt complexes are presented together with characteristic chromic behavior resulting from the modulation of the intermolecular interactions coupled with energetic fluctuation in the ground and excited states of the mesogens/chromophores.

EXPERIMENTAL SECTION

General Procedures. 1,2-Benzenedithiol ($BdtH_2$) was purchased from Aldrich Chemical. 1-Mercaptophenol ($HtpH_2$) was purchased from Tokyo Chemical Industry Co., Ltd. 4,4′-Di-(3-octyltridecyl)-2,2′-bipyridine (C8,10bpy), [$PtCl_2$(C8,10bpy)], and [Pt(Cat)(C8,10bpy)] (**1**) were synthesized by the literature methods.[3a] All of the solvents for the synthesis and the measurements were distilled by standard methods under dinitrogen atmosphere. All synthetic operations were performed under dinitrogen atmosphere using Schlenk line techniques.

Synthesis. *[Pt(Htp)(C8,10bpy)] (**2**).* An 8 mL portion of CH_2Cl_2 and an 8 mL portion of MeOH were added to a mixture of $HtpH_2$ (64.7 mg, 0.513 mmol), NaOH (48.3 mg, 1.21 mmol), and [$PtCl_2$(C8,10bpy)] (407.3 mg, 0.4028 mmol). The mixture was heated at 40 °C for a day, affording a deep violet solution. Addition of 40 mL of MeOH afforded violet precipitates. The product was filtered and washed with MeOH, dissolved in 10 mL of CH_2Cl_2, and filtered. Removal of solvent by evaporation yielded a violet oil. yield 400.6 mg (0.376 mmol, 93%). FAB-MS: m/z 1065 [$M^+ + 1$]. ^{1}H NMR (CD_2Cl_2, 500 MHz): δ = 9.33 (d, 1H, J = 6.0 Hz), 8.93 (d, 1H, J = 6.0 Hz), 7.81 (d, 1H, J = 1.5 Hz), 7.75 (d, 1H, J = 1.5 Hz), 7.52 (dd, 1H, J = 6.0, 1.5 Hz), 7.17 (dd, 1H, J = 7.5, 1.5 Hz), 7.15 (dd, 1H, J = 6.5, 1.5 Hz), 6.69 (m, 2H), 6.43 (m, 1H), 2.76 (t, 2H, J = 8.0 Hz), 2.70 (t, 2H, J = 8.3 Hz), 1.70 (m, 2H), 1.64 (m, 2H), 1.40−1.24 (m, 66H), 0.88 (t, 12H, J = 7.0 Hz). Calcd for $C_{58}H_{98}N_2O_2SPt$: C, 64.35; H, 9.12; N, 2.59. Found: C, 64.74; H, 9.04; N, 2.61. The sample is hygroscopic, including one water molecule.

*[Pt(Bdt)(C8,10bpy)] (**3**).* The complex was synthesized using a procedure similar to that for **2**, using $BdtH_2$ (69.3 mg, 0.487 mmol), NaOH (63.0 mg, 1.58 mmol), and [$PtCl_2$(C8,10bpy)] (448 mg, 0.443 mmol). The reaction was carried out at 85 °C for 1 h. Yield 417.0 mg (0.385 mmol, 87%). FAB-MS: m/z 1,080 [$M + 1$]$^+$. ^{1}H NMR (CD_2Cl_2, 500 MHz): δ = 9.10 (d, 2H, J = 5.5 Hz), 7.87 (d, 2H, J = 1.5 Hz), 7.35 (dd, 2H, J = 5.5, 1.5 Hz), 7.32 (dd, 2H, J = 6.0, 3.5 Hz), 6.75 (dd, 2H, J = 6.0, 3.5 Hz), 2.73 (m, 4H), 1.68 (m, 4H), 1.40−1.24 (m, 66H), 0.88 (t, 12H, J = 9.0 Hz). Calcd for $C_{58}H_{96}N_2S_2Pt$: C, 64.47; H, 8.95; N, 2.59. Found: C, 64.41; H, 8.90; N, 2.64.

Physical Measurements. ^{1}H NMR spectroscopy was performed using a JEOL A-500 spectrometer. Mass spectra were recorded using a JEOL JMS-HX110A mass spectrometer. Elemental analyses were carried out on a Thermo Finnigan Instrument Flash EA 112 series. Microphotographs were taken by an Olympus BX51 polarizing microscope equipped with a DP70 digital camera. The samples were cooled and heated on a Linkam THM600 hot stage with programmable temperature controllers L-600A and LK600PM under N_2 atmosphere. Variable temperature X-ray powder diffraction measurements were carried out with Cu Kα radiation equipped with a Rigaku Ultima IV or a Rigaku RINT-2000 diffractometer using Al sample pans. Differential scanning calorimetry measurements were performed on a METTLER DSC822e under N_2 flow. Samples were placed between an aluminum DSC pan and lid. Electrochemical measurements were carried out with an ALS model 650A electrochemical analyzer. A standard three-electrode system (a glassy carbon working electrode, platinum-wire counter electrode, and $Ag/Ag^+/CH_3CN$ electrode as reference) was used for CV studies in solution. Absorption spectra in solution were measured by a Shimazu MultiSpec-1500 or a Hitachi U-3500 spectrophotometer. Temperature-dependent absorption spectra for the condensed phases were measured with a JASCO MSV-370 UV−vis spectrometer. The samples were placed on a quartz plate in a Linkam THM600 hot stage with programmable temperature controller L-600A and LK600PM under N_2 atmosphere. Emission spectra in solution were collected with a JASCO FP-6600 spectrometer under Ar or N_2 atmosphere with a quartz cell. Emission spectra in the frozen solvents at 77 K were measured using a quartz tube, and all solvents were degassed before use. For temperature-dependent emission spectra for the condensed phases, the samples were directly fixed to the inside of a quartz cell and cooled with liquid N_2/MeOH mixtures in a dewar, and temperatures were monitored with a thermocouple. ESR spectrum was recorded with a JEOL RE-3X spectrometer operating at room temperature. All measurements for the condensed phases were carried out after cooling the isotropic liquid phases to minimum temperatures in the hotstage.

RESULT AND DISCUSSION

Synthesis. The liquid crystalline complexes shown in Scheme 1, [Pt(Cat)(C8,10bpy)] (**1**), Pt(Htp)(C8,10bpy)] (**2**), and [Pt(Bdt)-(C8,10bpy)] (**3**), were synthesized by common synthetic procedures. The complexation of redox-active ligand with a precursor complex, [$PtCl_2$(C8,10bpy)], in the presence of bases affords deeply colored, sticky materials in efficient, high yields. The complexes **1**−**3** have asymmetric molecular structures derived from redox-active ligands and C8,10bpy bound at the opposite sites. Therefore, the complexes possess relatively large dipole

dx.doi.org/10.1021/ic102123n |*Inorg. Chem.* 2011, 50, 4279–4288

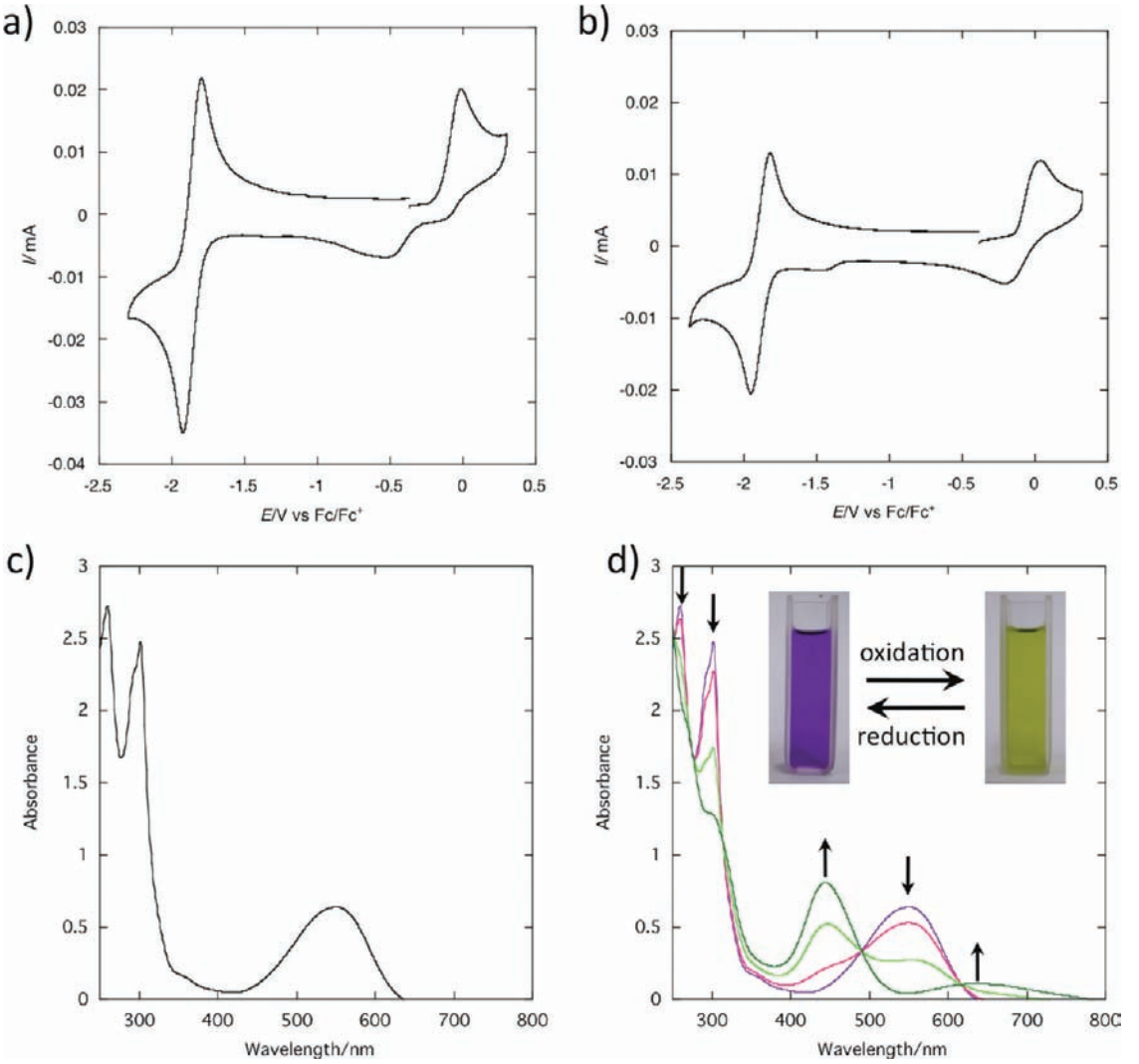

Figure 1. Cyclic voltammograms of (a) **2** and (b) **3** in CH_2Cl_2 (200 mV/s, 0.1 M *n*-Bu_4NPF_6, under N_2). (c) Absorption spectrum of **3** in CH_2Cl_2. (d) Absorption spectral changes during the oxidation process of **3** at 0.2 V vs Fc/Fc^+. The inset pictures show the violet, neutral state (right) and the green, oxidized state (left), respectively.

moments modulated by the nature of coordinating atoms. The polar nature plays a key role in stabilizing the LC phase as well as their spectro- and electrochemical properties, as described below.

Redox Properties of 2 and 3. As complex **1** shows,[3a] newly synthesized **2** and **3** are expected to give characteristic redox activity in solution. Figure 1a,b displays cyclic voltammograms of **2** and **3** measured in dichloromethane. Complexes **2** and **3** commonly undergo quasireversible one-electron reduction at −1.86 and −1.89 V vs Fc/Fc^+ for **2** and **3**, respectively, corresponding to C8,10bpy-based reduction processes, which was also found for **1** at −1.87 V (Table 1).[3a] The reduction potentials seem not to be affected by the nature of Cat, Htp, and Bdt, suggesting rigidity of the LUMO levels in **1**−**3**. In contrast to common features of the reduction processes of **1**−**3**, remarkable differences depending on the nature of the coordinating atoms are found in oxidation processes for **1**−**3**. As previously reported, complex **1** shows a reversible one-electron oxidation process on the Cat to produce a monoanionic, paramagnetic species, $[Pt(SQ)(C8,10bpy)]^+$ at $E_{1/2}$ = −0.01 V.[3a] On the other hand, complexes **2** and **3** exhibit first anodic pekas at −0.01 (**2**) and 0.01 (**3**) V with poor

Table 1. Electrochemical Data of 1−3 in CH_2Cl_2

complex	$E^{red}_{1/2}$	$E^{ox}_{1/2}$	E^{ox}_{pa}	E^{ox}_{pc1}	E^{ox}_{pc2}
1[a]	−1.87	−0.01	0.06	−0.08	
2[b]	−1.86		−0.01	−0.11	−0.51
3[b]	−1.89		0.01	−0.16	

[a] Reference 3a (V vs Fc/Fc^+; conditions: in CH_2Cl_2, 100 V/s, 0.1 M *n*-Bu_4NClO_4, under N_2). [b] V vs Fc/Fc^+. Conditions: 200 mV/s, 0.1 M *n*-Bu_4NPF_6, under N_2.

electrochemical reversibility dissimilar to that of **1**. Upon negative scans, complex **2** shows two peaks in cathodic currents at −0.11 and −0.51 V, while that for **3** was observed at −0.16 V. The oxidation process of **3** demonstrates better electrochemical reversibility compared with that of **2**, but peak-to-peak separation of the first oxidation process is found to be 0.17 V, far from the theoretical value for an ideal one-electron transfer process. In addition, the shape of the voltammogram for the oxidation process is significantly asymmetric and scan rate dependent, indicating

dx.doi.org/10.1021/ic102123n |*Inorg. Chem.* 2011, 50, 4279–4288

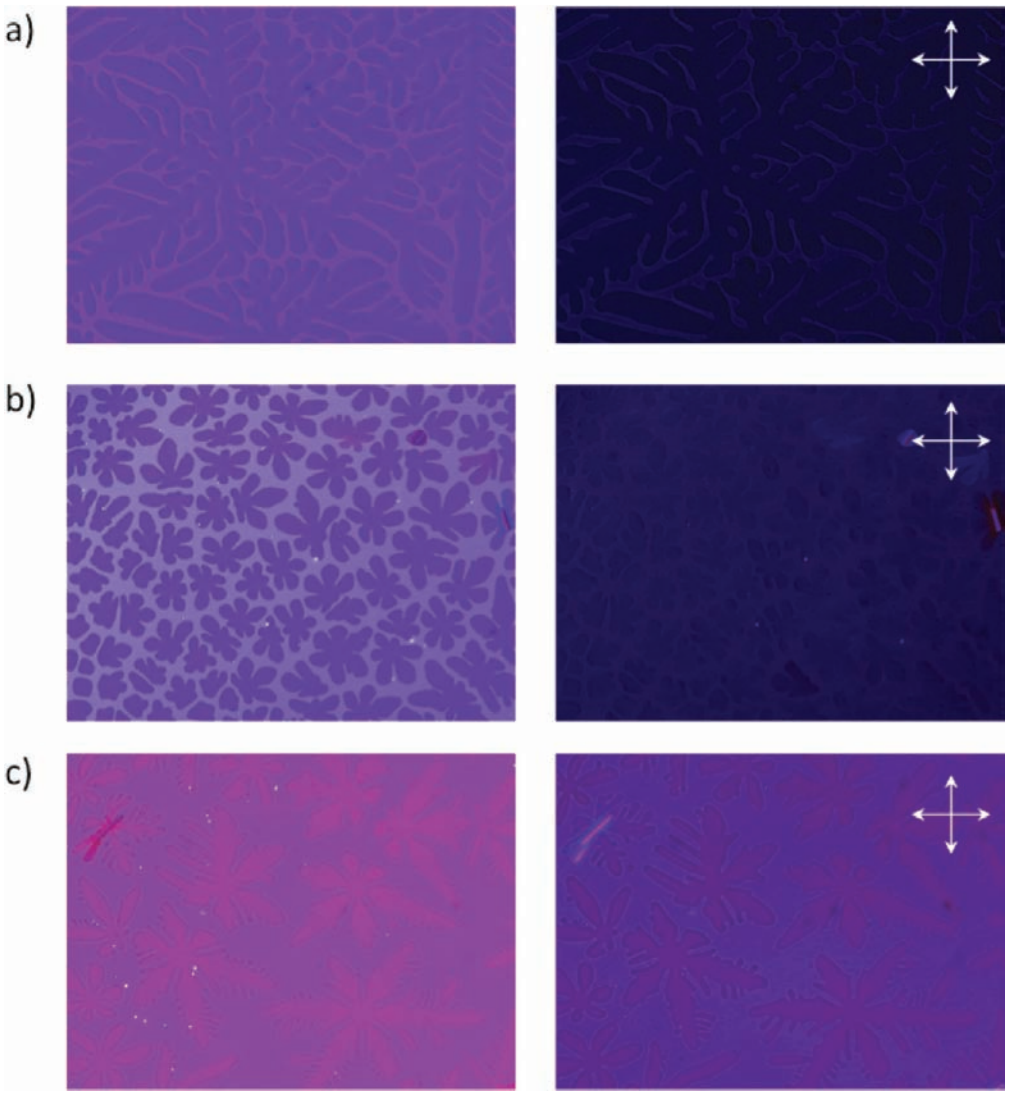

Figure 2. Polarized optical microscope images of thin films between two glass slides taken at (a) 185 (**1**), (b) 170 (**2**), and (c) 175 (**3**) °C under parallel (left) and crossed (right) polarizers.

electrochemical irreversibility within the experiment time scale (see Figure S1 in the Supporting Information). Similar electrochemical behavior was observed in well-defined dithiolato-containing metal complexes.[6] Although complete characterization of the oxidized species for **1**−**3** are still in progress, the following spectroelectrochemical and ESR experiments performed for **3** in CH_2Cl_2 solution gave us more insight in the nature of the oxidized species. A UV−vis absorption spectrum of **3** in CH_2Cl_2 solution is shown in Figure 1c. Two intense narrow bands are observed in the UV region at 260 nm ($\varepsilon = 33\,800\ M^{-1}\ cm^{-1}$) and 304 nm ($\varepsilon = 28\,900\ M^{-1}\ cm^{-1}$). The lower energy band was assigned to $\pi-\pi_1^*$ transition localized on the bpy moieties, while the higher energy band is associated with the $\pi-\pi_2^*$ transition.[7] At longer wavelengths, a shoulder is resolved near 350 nm ($\varepsilon = 2490\ M^{-1}\ cm^{-1}$), which is consistent with a MLCT (dπ-to-π^*(bpy)) transition. A very broad and solvent sensitive band (vide infra) occurs at longer wavelengths, 556 nm ($\varepsilon = 7170\ M^{-1}\ cm^{-1}$). A similar band was observed in the spectra of numerous platinum(II) dithiolato diimine complexes and can be described as a mixed-Pt/Bdt-to-bpy charge transfer (MMLL′CT) transition.[7] Figure 1d demonstrates the absorption spectral changes during the electrochemical oxidation of **3** in CH_2Cl_2 at 0.2 V. The oxidation led to the color changes of the solution from violet (neutral form) to light green (oxidized form). The presence of isosbestic points at 252, 271, 313, 490, and 617 nm and a reversible color change clearly demonstrate that electrochemical oxidation of **3** takes place through a chemically reversible process. Interestingly, in situ ESR measurements revealed that the oxidation of **3** provided a product with ESR-silent, diamagnetic character. A corresponding behavior was observed and suggested a fast intermolecular process of the radical species.[6a]

LC Structures and Phase Diagrams of 2 and 3. Complex **1** with the Cat is fairly stable under ambient conditions both in solution and in the condensed states. In contrast, the solutions of **2** and **3** with at least one coordinating sulfur atoms exhibit moderate stability in solution, where solution gradually changed from violet to yellow under atmosphere and natural light irradiation. The oxygenation of the coordinating sulfur atoms has been known to be responsible for these transformations in the presence of light and oxygen.[7,8]

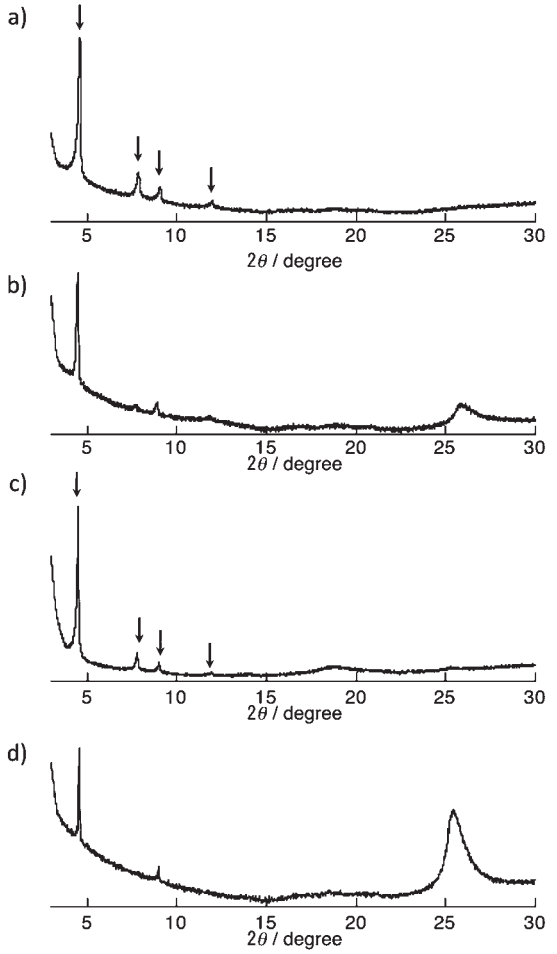

Figure 3. XRD patterns of the Col_{ho} phases of **2** during (a) first heating and (b) first cooling processes and those of **3** during (c) first heating and (d) first cooling processes at 35 °C.

Table 2. Phase Diagrams for 1−3

complex	phase [°C (kJ/mol)]
1[a]	G −62 × 31 (3.9) Col_{ho} 195 (1.3) Iso
2[b]	G −62 X1 −46 (0.5) X2 −35 (0.8) Col_{ho} 186 (1.5) Iso
3	G −58 X −18 (8.8) Col_{ho} 194 (2.2) Iso

[a] Reference 3a. [b] The measurements were carried out after drying the sample at 60 °C.

The thermal phase transition behaviors of **2** and **3** were examined by polarized optical microscopy (POM), differential scanning calorimetry (DSC), and variable temperature X-ray diffraction (XRD) experiments. All of the virgin samples precipitated from solutions that remain highly viscous until they clear into an isotropic liquid (Iso) at 195, 186, and 194 °C for **1**, **2** and **3**, respectively. Successive cooling initiated the growth of dendritic textures with 6-fold symmetry as shown in Figure 2. At the beginning of growths, these complexes commonly exhibit spontaneous homeotropic alignment between two untreated glasses as can be seen from the dark images under closed polarizing conditions. Upon the cooling to room temperature the films exhibit birefringence with decreasing temperatures (see Figures S2−S4 in the Supporting Information).

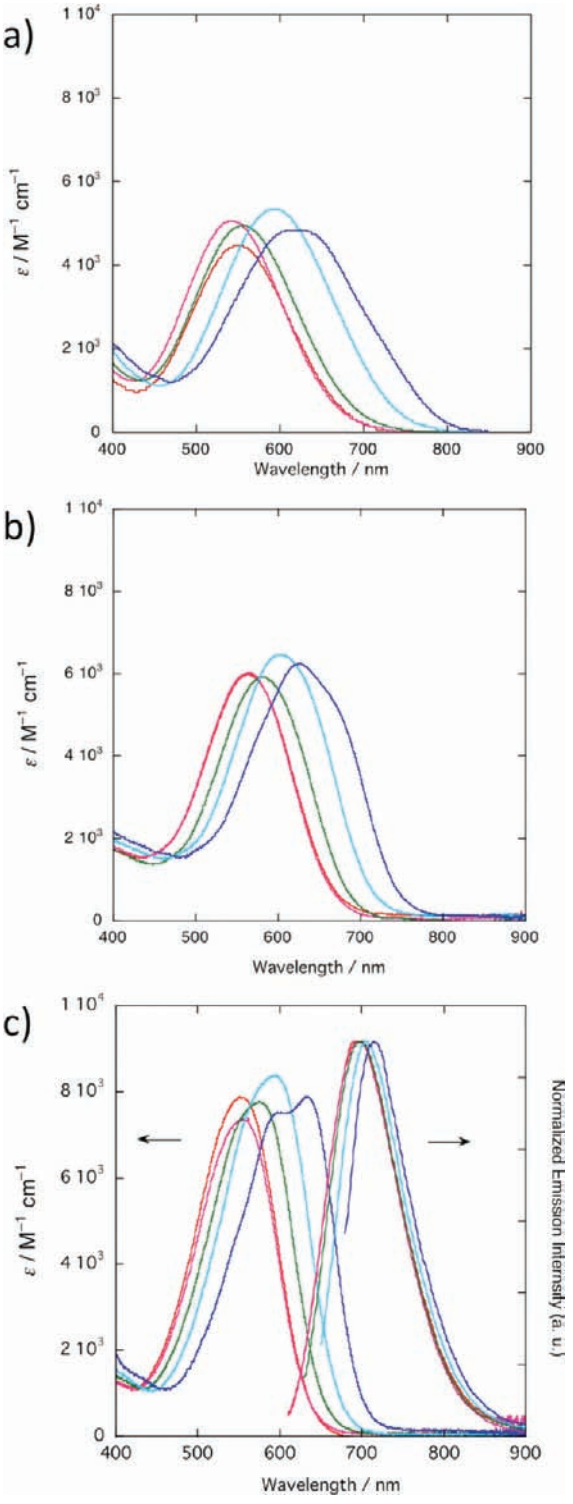

Figure 4. Absorption spectra of (a) **1** and (b) **2** and absorption and emission spectra of (c) **3** in acetone (red line), dichloromethane (pink line), chloroform (green line), THF (sky blue line), and benzene (blue line) at room temperature. The concentration of solutions, absorption coefficients, and the excitation wavelengths for emission spectra are listed in Tables 3 and 4.

Complexes **2** and **3** revealed their assembled structures through the XRD patterns shown in Figure 3. Sharp reflections in the low angle region with relative positions $1:(^1/_3)^{1/2}:^1/_2:(^1/_7)^{1/2}$ are

dx.doi.org/10.1021/ic102123n |*Inorg. Chem.* 2011, 50, 4279–4288

characteristic for a two-dimensional hexagonal lattice with the lattice parameters of a_{hex} = 20.4 and 19.4 Å for **2** and **3**, respectively, at 35 °C. In addition to the reflections from the molten alkyl chains, the characteristic reflections appear at around 26° with a *d*-spacing of approximately 3.5 Å. These reflections strongly indicate that the complexes possess weakly ordered short-range structures within the columns. As a whole, the XRD patterns clearly demonstrate that complexes **2** and **3** form a hexagonal columnar ordered LC phase (Col_{ho}), as previously reported **1** (a_{hex} = 19.6 Å, d_{001} = 3.4 Å at 40 °C). The formation of the columns can be reproduced assuming a one-dimensional column constructed from the molecules aligned so as to cancel out their dipole moments within two or three or more molecules.

The Col_{ho} phases of **2** and **3** are thermally transformed to isotropic liquid phase (Iso) by heating, while unknown phases (X) with structures having higher orders are formed by cooling of the Col_{ho} phases (see Figures S2−S8 in the Supporting Information for POMs, variable temperature XRD, and DSC curves of **2** and **3**). Furthermore, both complexes commonly show glass transitions (G phase) of the branched alkyl tails around −60 °C, which were characterized by the appearance of thermal anomalies in the DSC curves. The phase transition behaviors of **1**−**3** are summarized and compared in Table 2. Moderate dependency was observed for the clearing points, 186 °C (**2**) < 194 °C (**3**) < 195 °C (**1**), among the unsubstituted complexes with different coordinating atoms. The net dipole moments account for the observed tendencies in the stability of the Col_{ho} phase; complex **2** has Htp with lower symmetry compared with Cat and Bdt,

Table 3. Absorption Spectral Data of the MMLL′CT Bands of 1−3 in Solvent Media

solvent	conc (× 10^{-5} mol/L)	λ_{abs}/nm (ε/M/cm)
	Complex **1**	
acetone	1.58	549 (4480)
dichloromethane	2.88	542 (5070)
chloroform	3.61	555 (4940)
THF	2.86	594 (5330)
benzene	2.27	619 (4850)
	Complex **2**	
acetone	3.12	564 (5990)
dichloromethane	2.95	564 (6010)
chloroform	3.09	579 (5920)
THF	2.86	602 (6470)
benzene	3.01	626 (6250), 670 (5230)
	Complex **3**	
acetone	2.91	557 (7840)
dichloromethane[a]	2.87	555 (7340)
chloroform	3.12	575 (7780)
THF	2.79	595 (8370)
benzene	3.02	600 (7490), 637 (7850)

[a] The data included in Table 1 was independently obtained with the experiments shown in Figure 1.

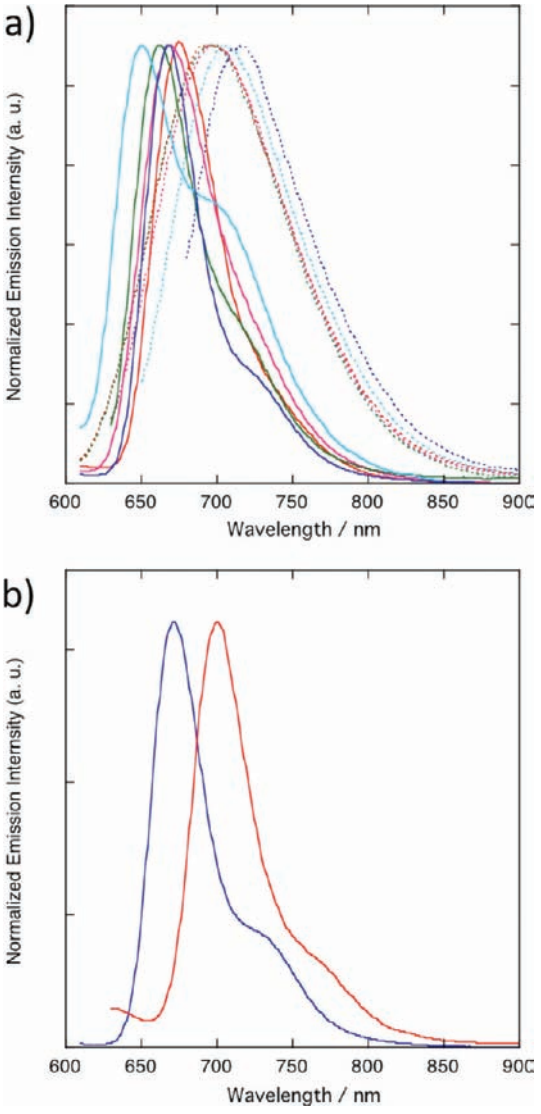

Figure 5. (a) Emission spectra of **3** in acetone (red line), dichloromethane (pink line), chloroform (green line), THF (sky blue line), and benzene (blue line) at room temperature (dotted lines) and 77 K (solid lines). (b) Emission spectra of **2** (red line) and **3** (blue line) in the G phases at 77 K. The concentration of solutions and the excitation wavelengths for emission spectra are listed in Table 4.

Table 4. Photoluminescence Properties of 3 in Solvent Media

	RT		77 K		
solvent	conc (×10^{-5} mol/L)	λ_{em}/nm (λ_{ex}/nm)	conc (×10^{-5} mol/L)	λ_{em}/nm (λ_{ex}/nm)	rigidochromic shift (cm^{-1})
acetone	2.91	695 (570)	2.93	675 (565)	427
dichloromethane	2.87	700 (570)	3.05	669 (555)	662
chloroform	3.12	699 (590)	3.28	662 (580)	800
THF	2.79	705 (610)	2.97	650 (570)	1201
benzene	3.02	716 (640)	3.02	668 (570)	1003

dx.doi.org/10.1021/ic102123n |*Inorg. Chem.* 2011, 50, 4279–4288

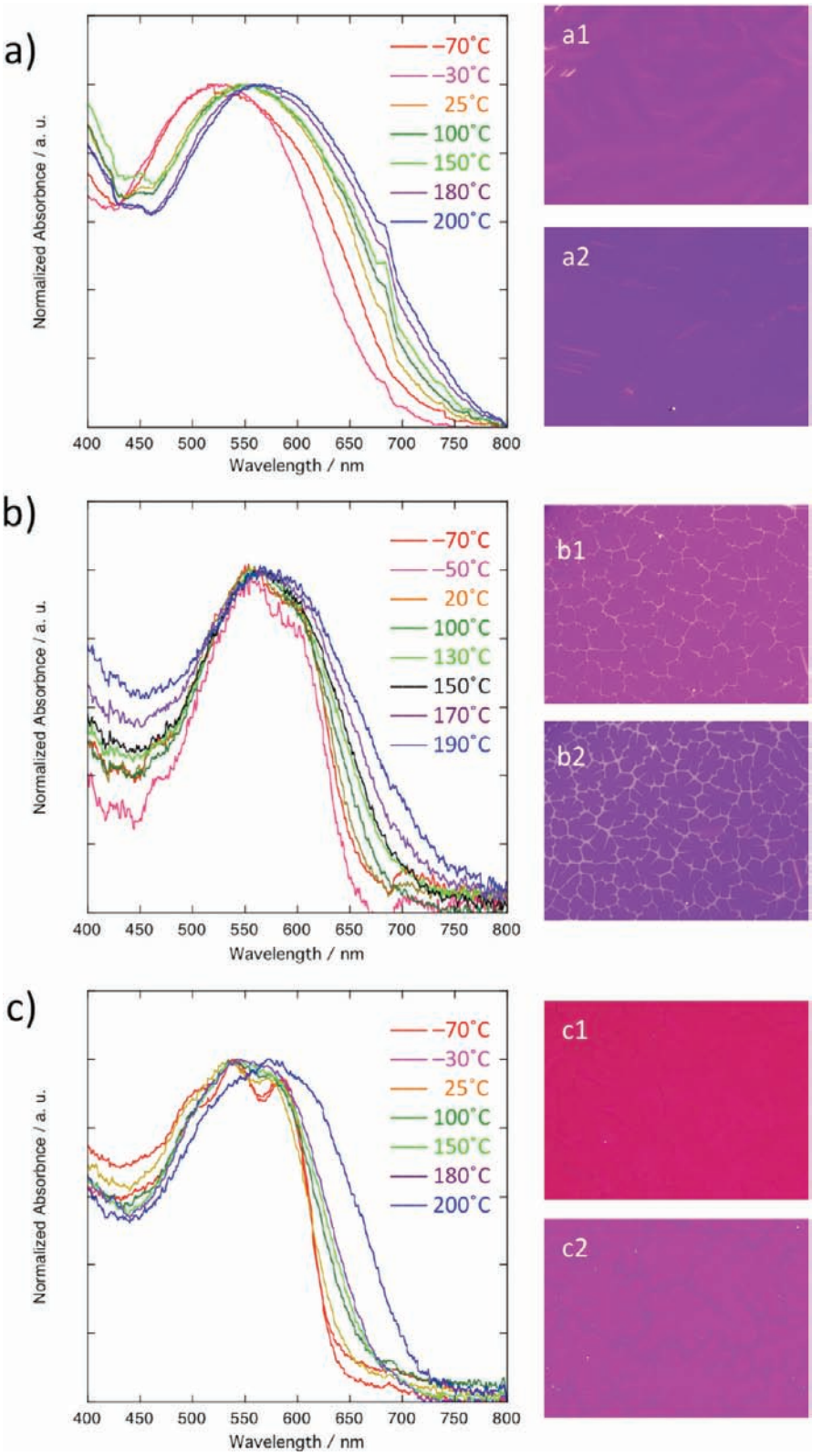

Figure 6. Temperature-dependent absorption spectra of (a) **1** (a1, 35 °C; a2, 150 °C), (b) **2** (b1, 35 °C; b2, 150 °C), and (c) **3** (c1, 35 °C; c2, 150 °C) in the Col_{ho} and Iso phases on heating processes. The pictures show the thermochromic behaviors of the complexes in the Col_{ho} phases.

leading to weaker dipole···dipole interactions within the column. These assumptions were confirmed by solvatochromic shifts of **1**−**3** in several solvents (vide infra and also see Figures S9 and S10 in the Supporting Information). More pronounced effects of the coordinating atoms are found in the stability of the X phases. The most stable X phase is formed in **1**, whereas that of **2** is easily transferred to the Col_{ho} at −35 °C. As a result, complex **2** has the widest temperature range for the Col_{ho} phase. The

dx.doi.org/10.1021/ic102123n |*Inorg. Chem.* 2011, 50, 4279–4288

appearance of the single Col_{ho} phase in **1**−**3** over relatively wide temperature ranges allowed us to spectroscopically pursue these complexes by changing the temperature over approximately 200 °C, including ambient temperature. In addition, the degree of structural order/disorder of both central mesogens/chromophores and the branched alkyl chains would be differently modulated within the G, X, Col_{ho}, and Iso phases.

Solvatochromism of 1−3 in Solvent Media. It is important to compare the spectrochemical behaviors of the complexes in solvent media and in Col_{ho} phases, and also those of condensed phases derived from heating or cooling of the Col_{ho} phases. Figure 4 shows absorption spectra of **1**−**3** at room temperature dissolved in acetone, dichloromethane, chloroform, THF, and benzene with differing polarity, and the absorption spectral data are listed in Table 3. The complexes show characteristic absorption bands centered at between 542 and 670 nm. These bands clearly show solvent polarity-dependent chromism very similar to those of the related complexes.[9] A peak maximum of each band as well as an absorption onset is blue-shifted as solvent polarity increased by approximately 2500 cm^{-1} in energy, demonstrating negative solvatochromism.

The nature of the HOMO/LUMO orbitals and the ground and excited states of Cat and Bdt complexes with bpy coligand has been experimentally and theoretically investigated. The HOMO of **1** with the coordinating oxygen atoms has been known to localize on the Cat,[10] whereas that of complex **3** with the coordinating sulfur atoms possesses a hybridized HOMO contributed from the Bdt and Pt(II) atom.[9,10] Regarding the LUMO orbitals, all of the complexes commonly have a LUMO orbital localized on the bpy moieties as suggested also from the CV data; thus, the differences found in spectrochemical properties of **1**−**3** basically depend on the nature of the ground states. On the basis of these characters, the observed absorption bands could be assigned to a Cat-to-bpy charge transfer (LL′CT) and MMLL′CT band for **1** and **3**, respectively. Therefore, the common feature of the ground states of **1**−**3** is their polar ground states and nonpolar excited states generated by the MMLL′CT transitions. Because the polar ground states could strongly interact with polar solvent molecules through dipole···dipole couplings, the stabilization of the ground states is enhanced with increasing solvent polarity. Thereby, the energy gap between the ground and excited states tends to be wider in acetone and narrower in benzene, respectively. Regarding the effects of coordinating atoms, the structures of the absorption bands of **1** and **2** are similar to each other, in which the bandwidths are remarkably broader than that of **3** as shown in Figure 4. These features, in particular the property to absorb light with longer wavelengths, influence the emission properties of the complexes in solution media (vide infra).

Solvato- and Rigido-Luminochromism of 3 in Solvent Media. In addition to these characteristic CT absorption bands from the ground states, complex **3** demonstrates phosphorescence from the excited states of the [Pt(Bdt)(bpy)] chromophore in region 695−716 nm in solvent media (Figure 4c and Table 4). The observed emission bands are well-known to originate from the MMLL′CT excited states,[9] although the emission band energy shows weak solvent polarity dependency compared with the absorption bands. The solvent dependency of the emission maxima of **3** is accounted for by the nonpolar nature of the excited states having a charge transfer character from the Pt/Bdt to the π^* orbital of bpy. As the temperature decreased to 77 K, the band structures of emission spectra of **3** in frozen

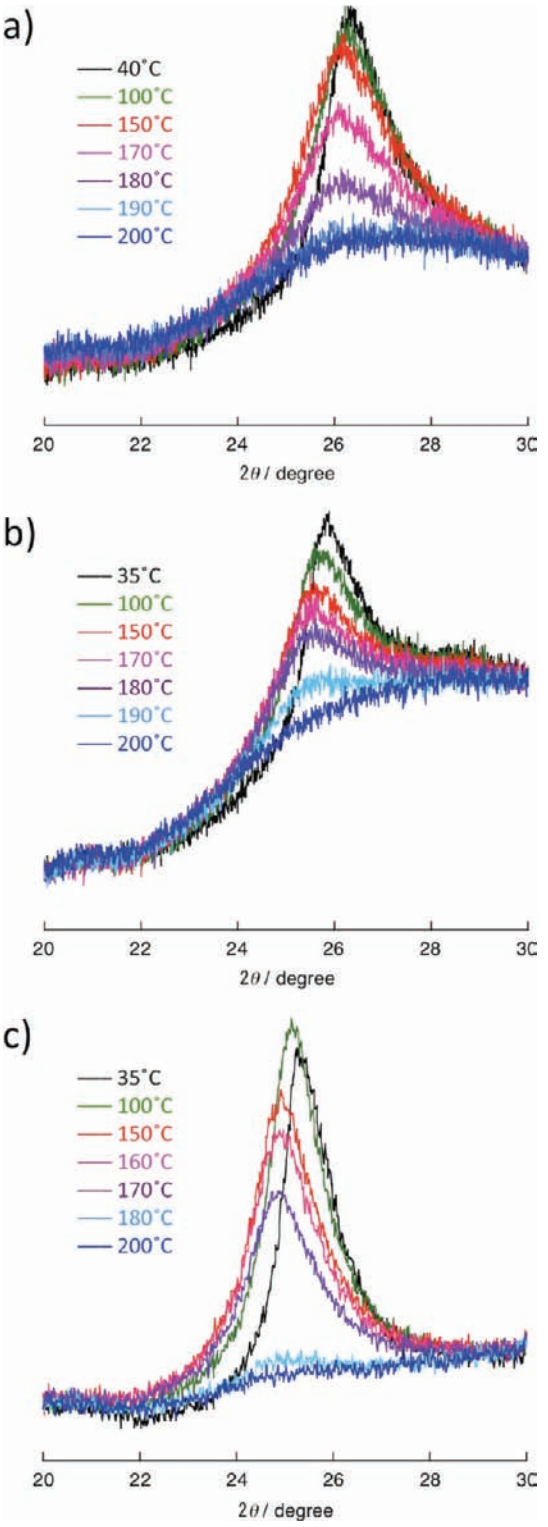

Figure 7. Temperature-dependent X-ray diffractograms from the (001) planes of (a) **1**, (b) **2**, and (c) **3**, on heating processes.

solvents are more pronounced [Figure 5a (solid lines)] than those at room temperature [Figure 5a (dashed lines)]. The shoulders were observed at longer wavelength edges separated from the strongest band by approximately 1100 cm^{-1}. Apparently, the emission bands suffer a common rigidochromic effect,[11] where the blue-shift of the bands in going from fluid

dx.doi.org/10.1021/ic102123n |*Inorg. Chem.* 2011, 50, 4279–4288

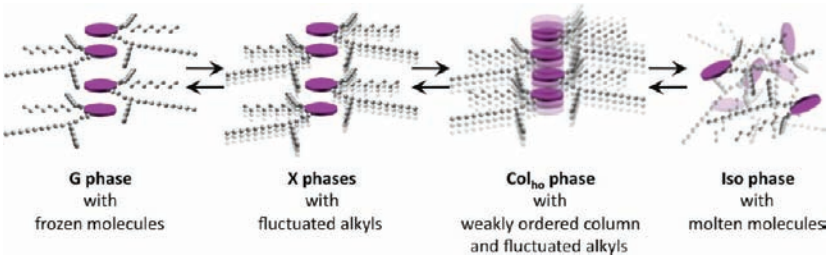

Figure 8. Schematic drawings of self-association of redox-active LCs and their phase transition behaviors with varying structural fluctuations.

solution to frozen solvents ranged from 427 cm^{-1} for acetone to 662, 800, and 1003 cm^{-1} for dichloromethane, chloroform, and benzene, respectively, and to a maximum shift of 1201 cm^{-1} for THF. Because of the low viscosity of the medium at room temperature, solvent molecules in the vicinity of the excited-state molecule readily undergo reorientation by the dipole···dipole interaction within the lifetime of the excited state, resulting in the formation of the fully relaxed excited state. Thus, the emissions at room temperature occur from the fully relaxed excited states. On the other hand, the excited states at 77 K emit before the solvent relaxation occurs, resulting in the rigidochromic effects on the emission spectra.

Luminescence in the Condensed Phases. Complex **1** is nonemissive both in solution and in the condensed phases over the whole temperature region. On the other hand, characteristic phosphorescence is found for **2** and **3** in the condensed phases, in particular at low temperatures (Figure 5b). Interestingly, complex **2** is emissive in the condensed phase, unlike its behavior in solution. When both complexes were cooled to 77 K, at which the G phases are commonly formed, the red emissions maximized at 701 and 672 nm appear with a shoulder at 770 and 720 nm for **2** and **3**, respectively, upon irradiation of 570 nm light. The structures and energies of the emission bands of **2** and **3** are found to be similar to those of **3** in frozen solvents at 77 K (solid lines in Figure 5a), indicating the same origins of the observed emissions.

Thermochromism in the Col$_{ho}$ Phases. Complexes **1**−**3** demonstrate the single Col$_{ho}$ phases over relatively wide temperature ranges over approximately 200 °C. Below room temperature, these complexes show nearly temperature-independent absorption spectra in the condensed phases, even though the Col$_{ho}$ to X (X1 for **2**) phase transitions occur at 31, −35, and −18 °C for **1**, **2**, and **3**, respectively. Upon the phase transitions to the G phases, each absorption peak in the X phases tends to be pronounced at −70 °C (Figure 6). In contrast, remarkable changes in the spectra were observed around 640−800 nm for **1**−**3** with increasing temperature, in particular, above 100 °C (Figure 6). These spectral changes lead to visible, thermochromic behavior of the complexes in the Col$_{ho}$ phases, as demonstrated in the photographs in Figure 6. All complexes, therefore, tend to show color changes from reddish violet to bluish violet coming from increased light absorption around 700 nm. It is noteworthy that the observed temperature-dependent spectra are quite similar to the spectroscopic changes found in solvatochromism in going from the polar acetone to the nonpolar benzene (Figure 4). The increases in absorbing light with longer wavelengths commonly occur by heating in the condensed phases as by decreasing a polarity of solvent.

To understand the origin of the thermochromic behaviors in terms of structural factors, temperature-dependent XRD studies were carried out. The most prominent temperature dependency was observed in (001) diffractions that appeared around 26° for all of the complexes (Figure 7). These reflections can be regarded as an index to evaluate the environment of the central mesogens/chromophores, because they originate from the stacking interactions of the polar mesogens/chromophores. Importantly, these diffractions commonly show broadening as the temperature increases as well as shifting toward smaller 2θ (Figure 7), implying increases in the degrees of disorders in the column and the lengthening of the mean plane distances between the stacked molecules. For a more quantitative analysis on the extent of order/disorder within the Col$_{ho}$ phases, the correlation length, l, a measure of the length scale of the positional order, was calculated using the Scherrer equation $l = 0.9\lambda/w_{1/2} \cos\theta$,[12] where λ is the wavelength of the incident X-ray beam (Cu Kα = 1.54 Å). $w_{1/2}$ is the full-width at half-maximum (fwhm) of the reflection, and the diffraction angle θ is the maximum of the reflection. Both values are easily determined after fitting the X-ray patterns, and the correlation lengths were estimated to be ca. 60 Å for **1** (40 °C), **2** (35 °C), and **3** (35 °C). Interestingly, the correlation lengths decrease with increasing temperatures, while the fwhm values tend to increase as temperatures increase. The temperature dependent XRD measurements lead us to believe that approximately 20 molecular units are correlated around room temperature with weaker structural fluctuation, whereas the number of correlated molecules tends to decrease upon heating, affording stronger structural fluctuation within the column. Therefore, it is most reasonable to understand that the observed thermochromism originates from thermally induced fluctuations of the intermolecular interactions between the central half-disk-shaped mesogens/chromophores. Taking all of these spectral data into account, the observed thermochromism is driven by the destabilization of the ground state caused by thermal melting of the self-association in the column constructed from the dipolar couplings between the central mesogens/chromophores.

CONCLUSION

Figure 8 summarizes the observed thermochromic behaviors coupled with thermally induced structural fluctuations in **1**−**3**. In the G phases, all structural fluctuations within the mesogens/chromophores, as well as the alkyl chains, are frozen. The spectroscopic properties in the G phases and those in frozen solvents are similar to each other, indicating suppressed molecular motions in both the ground and excited states. Upon heating, the frozen alkyl chains tend to be molten, while the order of the mesogens/chromophores remains to be frozen. The dipolar couplings of the mesogens/chromophores are gradually weakened

upon further increase in temperature. Although the melting of the alkyl chains together with mesogens/chromophores leads to the decrease in the relative intensity of emission, the increase in thermal fluctuation of the mesogens/chromophores afforded the thermochromic behavior of **1**−**3**. Finally, complexes **1**−**3** lose all of the structural orders at the clearing points to give the Iso phases having the minimum light absorption energy. It is of interest to compare the absorption spectra of the Iso phases (blue lines in Figure 6) and those measured in benzene (blue lines in Figure 4). The similarity in these spectra indicates that complexes could have the minimized energetic gap between the ground and the excited states in the Iso phases among the observed condensed phases (G, X, Col_{ho}, and Iso) and in benzene among the five solvent media, although the Iso phase and benzene media would afford different chemical environments around the mesogens/chromophores. The self-association of the polar mesogens/chromophores would be enhanced by the coexistence with the long alkyl chains both in solvent media and in the condensed phases. This study clearly demonstrates that the natures of the ground and excited states of the molecular assemblies can be tuned not only by the coordinating atoms, as proven in the pioneering works,[5,6] but also by control of the self-association and structural fluctuations of the mesogens/chromophores themselves.

■ ASSOCIATED CONTENT

Supporting Information. Scan rate dependency of CVs for **1**−**3** (Figure S1), POMs (Figures S2−S4), variable temperature XRD (Figures S5−S7) of **1**−**3**, DSC curves (Figure S8) of **2** and **3**, plots of CT band energy vs [Pt(NN)(SS)] solvent parameter and E_T solvent scale for **1**, **2**, and **3** (Figure S9), and the photographs of solvatochromism of **1**−**3** (Figure S10). This material is available free of charge via the Internet at http://pubs.acs.org.

■ AUTHOR INFORMATION

Corresponding Author
*E-mail: chang@sci.hokudai.ac.jp.

■ ACKNOWLEDGMENT

This work was financially supported in part by a Grand-in-Aid for Scientific Research for Priority Area "Coordination Programming" (Area No. 2107) and the project for the Effective Utilization of Elements from the Ministry of Education, Culture, Sports, Science and Technology, Japan.

■ REFERENCES

(1) (a) *Metallomesogens: Synthesis, Properties and Applications*; Serrano, J. L., Ed.; Wiley-VCH: Weinheim, 1996. (b) Donnio, B.; Guillon, D.; Deschenaux, R.; Bruce, D. W. *Metallomesogens. Compr. Coord. Chem. II* **2004**, *7*, 357–627.(c) *Handbook of Liquid Crystals*; Demus, D., Goodby, J., Gray, G. W., Spiess, H.-W., Vill, V., Eds.; Wiley-VCH: Weinheim, Germany, 1998. (d) Goodby, J. W.; Mehl, G. H.; Saez, I. M.; Tuffin, R. P.; Mackenzie, G.; Auzély-Velty, R.; Benvegnu, T.; Plusquellec, D. *Chem. Commun* **1998**, 2057–2070. (e) Tschierske, C. *J. Mater. Chem.* **2001**, *11*, 2647–2671. (f) Chisholm, M. H. *Acc. Chem. Res.* **2000**, *33*, 53–61. (g) Bruce, D. W. *Acc. Chem. Res.* **2000**, *33*, 831–840. (h) Schmidt-Mende, L.; Fechtenkotter, A.; Müllen, K.; Moons, E.; Friend, R. H.; MacKenzie, J. D. *Science* **2001**, *293*, 1119–1122. (i) Martin, J. D.; Keary, C. L.; Thornton, T. A.; Novotnak, M. P.; Knutson, J. W.; Folmer, J. C. W. *Nat. Mater.* **2006**, *5*, 271–275. (j) Luk, Y.-Y.; Abbott, N. L. *Science* **2003**, *301*, 623–626.

(2) (a) Komatsu, T.; Ohta, K.; Fujimoto, T.; Yamamoto, I. *J. Mater. Chem.* **1994**, *4*, 533–536. (b) Ohta, K.; Moriya, M.; Ikejima, M.; Hasebe, H.; Fujimoto, T.; Yamamoto, I. *Bull. Chem. Soc. Jpn.* **1993**, *66*, 3553–3558. (c) Ohta, K.; Ikejima, M.; Moriya, M.; Hasebe, H. *J. Mater. Chem.* **1998**, *8*, 1971–1977. (d) Horie, H.; Takagi, A.; Hasebe, H.; Ohta, K. *J. Mater. Chem.* **2001**, *11*, 1063–1071.

(3) (a) Chang, H.-C.; Shiozaki, T.; Kamata, A.; Kishida, K.; Ohmori, T.; Kiriya, D.; Yamauchi, T.; Furukawa, H.; Kitagawa, S. *J. Mater. Chem.* **2007**, *17*, 4136–4138. (b) Yazaki, S.; Funahashi, M.; Kato, T. *J. Am. Chem. Soc.* **2008**, *130*, 13206–13207. (c) Carano, M.; Chuard, T.; Deschenaux, R.; Even, M.; Marcaccio, M.; Paolucci, F.; Prato, M.; Roffa, S. *J. Mater. Chem.* **2002**, *12*, 829–833. (d) Swarts, J. C.; Langner, E. H. G.; Krokeide-Hove, N.; Cook, M. J. *J. Mater. Chem.* **2001**, *11*, 434–443. (e) Deschenaux, R.; Schweissguth, M.; Levelut, A.-M. *Chem. Commun.* **1996**, 1275–1276.

(4) (a) Pierpont, C. G.; Lange, C. W. *Prog. Inorg. Chem.* **1994**, *41*, 331–442. (b) Pierpont, C. G. *Coord. Chem. Rev.* **2001**, *216*−*217*, 99. (c) Chang, H.-C.; Kitagawa, S. *Angew. Chem., Int. Ed.* **2002**, *41*, 130–133.

(5) Ray, K.; Petrenko, T.; Wieghardt, K; Neese, F. *Dalton Trans.* **2007**, 1552–1566.

(6) (a) Pap, J. S.; Benedito, F. L.; Bothe, E.; Bill, E.; George, S. D.; Weyhermüller, T.; Wieghardt, K. *Inorg. Chem.* **2007**, *46*, 4187–4196. (b) Geary, E. A. M.; Hirata, N.; Clifford, J.; Durrant, J. R.; Parsons, S.; Dawson, A.; Yellowless, L. J.; Robertson., N. *Dalton Trans* **2003**, 3757–3762.

(7) Connick, W. B.; Gray, H. B. *J. Am. Chem. Soc.* **1997**, *119*, 11620–11627.

(8) Matthew, T.; Bachman, R. E. *Inorg. Chem.* **2001**, *40*, 1550–1556.

(9) (a) Hissler, M.; McGarrah, J. E.; Connick, W. B.; Geiger, D. K.; Cummings, S. D.; Eisenberg, R. *Coord. Chem. Rev.* **2000**, *208*, 115–137. (b) Paw, W.; Cummings, S. D.; Mansour, M. A.; Connick, W. B.; Geiger, D. K.; Eisenberg, R. *Coord. Chem. Rev.* **1998**, *171*, 125–150. (c) Sakamoto, R.; Murata, M.; Kume, S.; Sampei, H.; Sugimoto, M.; Nishihara, H. *Chem. Commun.* **2005**, 1215–1217. (d) Islam, A.; Sugihara, H.; Hara, K.; Singh, L. P.; Katoh, R.; Yanagida, M.; Takahashi, Y.; Murata, S.; Arakawa, H. *Inorg. Chem.* **2001**, *40*, 5371–5380. (e) Connick, W. B.; Geiger, D.; Eisenberg, R. *Inorg. Chem.* **1999**, *38*, 3264–3265. (f) Cummings, S. D.; Eisenberg, R. *J. Am. Chem. Soc.* **1996**, *118*, 1949–1960. (g) Vanhelmont, F. W. M.; Johnson, R. C.; Hupp, J. T. *Inorg. Chem.* **2000**, *39*, 1814–1816. (h) Makedonas, C.; Mitsopoulou, C. A.; Lahoz, F. J.; Balana, A. I. *Inorg. Chem.* **2003**, *42*, 8853–8865. (i) Makedonas, C.; Mitsopoulou, C. A. *Spectrochim. Acta, Part A* **2006**, *64*, 918–930. (j) Ghosh, P.; Begum, A.; Herebian, D.; Bothe, E.; Wieghardt, K. *Angew. Chem., Int. Ed.* **2003**, *42*, 563–567.

(10) (a) Kamath, S. S.; Uma, V.; Srivastava, T. S. *Inorg. Chim. Acta* **1989**, *166*, 91–98. (b) Makedonas, C.; Mitsopoulpou, C. A. *Inorg. Chim. Acta* **2007**, *360*, 3997–4009. (c) Zuleta, J. A.; Bevilaacqua, J. M.; Proserpio, D. M.; Harvey, P. D.; Eisenberg, R. *Inorg. Chem.* **1992**, *31*, 2396–2404.

(11) Wrighton, M.; Morse, D. L. *J. Am. Chem. Soc.* **1974**, *96*, 998–1003.

(12) (a) Kouwer, P. H. J.; Jager, W. F.; Mijs, W. J.; Picken, S. J. *Macromolecules* **2002**, *35*, 4322–4329. (b) Ebert, M.; Frick, G.; Baehr, C.; Wendorff, J. H.; Wüstefeld, R.; Ringsdorf, H. *Liq. Cryst.* **1992**, *11*, 293–309.